Supplementary Material for Downstream Effects of Upstream Causes

A Parametric g-formula formulation

In all of the analyses, the outcome model was parameterized within the g-formula as a linear model:

$$\mathrm{E}\left[Y_{3t}|\overline{A}_t = [0_{t-1} : a_t], \overline{O}_t = \overline{o}_t\right] = h(\overline{A}, \overline{O}, \beta) \tag{G1}$$

For example, the correctly specified h for the simulations is

$$\beta_0^g + \beta_1^g a_{2t} + \beta_2^g a_{1t} + \beta_3^g l_{12t} + \beta_4^g l_{22t} + \beta_5^g y_{3,t-1}.$$

The stability analyses varied which L covariates were included in h, but the parameterization of the exposure (a_{2t} and a_{1t}) was not modified.

The average potential outcome $\mathrm{E}\left[Y_{3t}([0_{t-1} : a_t])\right]$ can be linked to observed data in the following manner:

$$\begin{aligned}
&\mathrm{E}\left[Y_{3t}([0_{t-1} : a_t])\right] \qquad\qquad (\text{G2})\\
&= \mathrm{E}\left\{\mathrm{E}\left[Y_{3t}([0_{t-1} : a_t])|\overline{A}_{2t} = [0_{t-1} : a_t], \overline{L}_t = \bar{l}_t\right]\right\} \text{ (no unmeasured confounders)}\\
&= \mathrm{E}\left\{\mathrm{E}\left[Y_{3t}|\overline{A}_t = [0_{t-1} : a_t], \overline{L}_t = \bar{l}_t\right]\right\} \text{ (causal consistency)}
\end{aligned}$$

According to the parametric g-formula, models for each $\mathrm{f}_{l_{pjk}} = \mathrm{f}_{l_{pjk}|\bar{l}_{j-1,k-1}, \bar{a}_{j-1,k-1}}$ must be fit. However, as will be clear below, the parameters corresponding to non-space- or time-varying covariates cancel in a causal contrast. Hence, we need only fit a model for the conditional mean of L_{22t}, for which we used a standard linear model with expectation $\gamma_0^g + \gamma_1^g l_{12t} + \gamma_2^g l_{22,t-1} + \gamma_3^g a_{1t}$. By causal consistency, $\mathrm{E}[L_{22t}(a_{1t})] = \gamma_0^g + \gamma_1^g l_{12t} + \gamma_2^g l_{22,t-1} + \gamma_3^g a_{1t}$. Under this assumed parameterization, $\mathrm{E}[L_{22t}(a_{1t}) - L_{22t}(0)] = \gamma_3^g$.

Putting (G2) together with the model for $f_{l_{22t}}$ obtains:

$$
\begin{aligned}
&\mathrm{E}\left[Y_{3t}(0_{t-1}:a_t) - Y_{3t}(0_t)\right] \\
&= \mathrm{E}\left\{ \mathrm{E}\left[Y_{3t}(0_{t-1}:a_t) - Y_{3t}(0_t)\right] \middle| A_{1t}=0, A_{2t}=0_{t-1}:a_t, \overline{L}_{2t} \right\} \\
&= \mathrm{E}\left\{\beta_1^g a_{2t} + \beta_2^g a_{1t} + \beta_4^g [L_{22t}(a_{1t}) - L_{22t}(0)]\right\} \text{ (plugging in } h) \\
&= \beta_1^g a_{2t} + \beta_2^g a_{1t} + \beta_4^g \,\mathrm{E}\left\{\mathrm{E}[L_{22t}(a_{1t}) - L_{22t}(0) | A_{11}=a_{11}, L_{12t}, L_{22,t-1}]\right\} \\
&= \beta_1^g a_{2t} + \beta_2^g a_{1t} + \beta_4^g \gamma_3^g.
\end{aligned}
$$

When $a_t = (1,1)'$ for all t, $\mu^g = \frac{1}{n_t}\sum_{t=1}^{n_t} \mathrm{E}\left[Y_{3t}([0_{t-1}, a_t]) - Y_{3t}(0_t)\right] = \frac{1}{n_t}\sum_{t=1}^{n_t}[\beta_1^g + \beta_2^g + \beta_4^g \gamma_3^g]$.

B Closed form estimator for SNM parameters

Vansteelandt and Joffe (2014) show that a consistent estimator of β^s can found by solving estimating equations (eq. 33):

$$\sum_i \sum_t \sum_s \{\mathrm{d}_{st}(\overline{L}_{ist}, \overline{A}_{ist}) - \mathrm{E}[\mathrm{d}_{st}(\overline{L}_{ist}, \overline{A}_{ist}) | \overline{L}_{ist}, \overline{A}_{i,s-1,t-1}]\}\{U_{ist}(\beta^s) - \mathrm{E}[U_{ist}(\beta^s) | \overline{L}_{ist}, \overline{A}_{i,s-1,t-1}]\}$$

where $\mathrm{d}_{st}(\overline{L}_{ist}, \overline{A}_{ist})$ is chosen to be $\mathrm{E}[\partial U_{st}(\beta^s)/\partial \beta^s | \overline{L}_{ist}, \overline{A}_{ist}]$. This formulation is slightly different from Vansteelandt and Joffe in that we added an additional dimension s. Since our endogenous covariate is space-varying rather than time-varying, the blip process is indexed by s rather than t.

Let $\rho_{ist} = \mathrm{E}[\mathrm{d}_{st}(\overline{L}_{ist}, \overline{A}_{ist}) | \overline{L}_{ist}, \overline{A}_{i,s-1,t-1}]$ and $\lambda_{ist} = \mathrm{E}[U_{ist}(\beta^s) | \overline{L}_{ist}, \overline{A}_{i,s-1,t-1}]$, then:

$$
\begin{aligned}
&\sum_i \sum_t \left\{ [\mathrm{d}_{1t}(\overline{L}_{i1t}, \overline{A}_{i1t}) - \rho_{i1t}](U_{i1t}(\beta^s) - \lambda_{i1t}) + [\mathrm{d}_{2t}(\overline{L}_{i2t}, \overline{A}_{i2t}) - \rho_{i2t}](U_{i2t}(\beta^s) - \lambda_{i2t}) \right\} \\
&= \sum_i \sum_t \left\{ \left[\begin{pmatrix} A_{i2t} \\ 0 \end{pmatrix} - \rho_{i2t} \right] (U_{i1t}(\beta^s) - \lambda_{i1t}) + \left[\begin{pmatrix} A_{i2t} \\ A_{i2t} \end{pmatrix} - \rho_{i2t} \right] (U_{i2t}(\beta^s) - \lambda_{i2t}) \right\} \\
&= \sum_i \sum_t \left\{ \left[\begin{pmatrix} A_{i2t} \\ 0 \end{pmatrix} - \rho_{i2t} \right] (Y_{i3t} - \beta_1^s A_{i2t} - \lambda_{i1t}) \right. \\
&\qquad \left. + \left[\begin{pmatrix} A_{i2t} \\ A_{i2t} \end{pmatrix} - \rho_{i2t} \right] (Y_{i3t} - \beta_1^s A_{i2t} - \beta_2^s A_{i1t} - \lambda_{i2t}) \right\} \\
&= \sum_i \sum_t \left\{ \begin{pmatrix} B_{i2t}^0 (r_{i3t} - \beta_1^s A_{i2t}) + B_{i2t}^1 (r_i^0 - \beta_1^s A_{i2t} - \beta_2^s A_{i1t}) \\ B_{1it}^1 (r_i^1 - \beta_1^s A_{i2t} - \beta_2^s A_{i1t}) \end{pmatrix} \right\}.
\end{aligned}
$$

In the last line, we let $B_{ist} = A_{i2t} - \rho_{ist}^k$. Let $r_{ist} = Y_{i3t} - \lambda_{ist}^k$.

Let $C_i = \sum_t r_i^0 (B_{i2t}^0 + B_{i2t}^1)$, $D_i = \sum_t (B_{i2t}^0 A_{i2t} + B_{i2t}^1 A_{i1t})$, $E_i = \sum_t B_{i2t}^1 A_{i1t}$, $F_i = \sum_t B_{1t}^1 r_i^1$, $G_i = B_{i1t}^1 A_{i2t}$, and $H_i = \sum_t B_{i1t}^1 A_{i1t}$. Then β^s is the solution to:

$$
\sum_i \begin{pmatrix} C_i - \beta_1^s D_i - \beta_2^s E_i \\ F_i - \beta_1^s G_i - \beta_2^s H_i \end{pmatrix}
$$

which yields,

$$
\hat{\beta}_1^s = \frac{\sum_i E_i \sum_i F_i - \sum_i C_i \sum_i H_i}{\sum_i E_i \sum_i G_i - \sum_i D_i \sum_i H_i} \text{ and } \hat{\beta}_2^s = \frac{\sum_i D_i \sum_i F_i - \sum_i C_i \sum_i G_i}{\sum_i D_i \sum_i H_i - \sum_i E_i \sum_i G_i}
$$

where

$$\sum_i E_i \sum_i G_i \neq \sum_i D_i \sum_i H_i, \quad \sum_i E_i \neq 0.$$

C Simulation details

The nodes in the simulated study system were parameterized and generated according to the following distributions:

$$t = 0 \begin{cases} L_{110} & \sim N(21.5, 2.5) \\ L_{220} & \sim N(-2.8, 0.7) \\ A_{s0} & \sim Bern(0.1) \text{ for } s = 1, 2 \\ Y_{30} & \sim N(2.25, 1.25) \end{cases}$$

$$t = 1, 2, 3 \begin{cases} L_{11t} & \sim N(23 + 0.2L_{11,t-1}, 2) \\ A_{1t} & \sim Bern(\text{logit}^{-1}(-2.5 + 0.09L_{11t} + 0.025A_{1,t-1})) \\ L_{12t} & \sim N(6.75 + 0.75L_{11,t-1}, 1) \\ L_{22t} & \sim N(2 - 0.04L_{12t} + 0.04L_{22,t-1} + 0.3A_{1t}, 0.25) \\ A_{2t} & \sim Bern(\text{logit}^{-1}(-2.5 + 0.09L_{12t} + 0.1L_{22t} + 0.05A_{1t} + 0.025A_{2,t-1})) \\ Y_{3t} & \sim N(-5 + 1A_{s-1,t} + 0.5A_{s-2,t} + 0.025L_{1,s-1,t} + 0.5L_{2,s-1,t} + 0.35Y_{3,t-1}, 1) \end{cases}$$

Code for the simulations can be found in the updown R package of the Supplementary Materials.

D Stability analyses

In addition to estimating the target parameters using all possible combinations of settings of the cutpoint and space-varying confounding variables, we also modified the exposure and outcome models to include a temperature by flow interaction term in both outcome and exposure models. This resulted in a total of 1200 point estimates per method. If some component model failed to converge for a method, then the estimate attempt was considered a failure. Across all 3600 attempts, model fitting failed 272 times for the MSMs, 70 times for the SNMs, and zero times for the g-formula.

To check the stability for the primary results presented in Figure 5 to the simple imputation procedure described in the main text, a multiple imputation procedure was used. The `aregImpmute` function from the Hmisc R package (Harrell et al., 2017) was used to impute missing values using year, month, distance between sites, flow, temperature, pH, dissolved oxygen, and each of the NP species. Five complete datasets were generated using the predictive mean matching imputation method with the match='closest' option. Point estimates from the complete datasets were averaged and the corresponding estimated standard errors pooled using Rubin's rules (Rubin, 2004).

Figure 1 shows all the point estimates within (-6, 6) across all the model options. In two cases, estimates from an SNM were outside this range. The results in Figure 1 conform to the general patterns described in the main text. Figure 2 show all the point estimates along with the p-values using different test statistic distributions. In each panel, the point estimates are the same, but the significance clearly depends on the test statistic distribution. Figure 3 repeats Figure 5 from the main text using estimates based on the imputation procedure described above.

Figure 1: This figure shows the 3258 point estimates obtained across settings of the cut-point, space-varying confounding variables, and exposure and outcome models. Point estimates for NO_3 between 86 and 109 km upstream are positive across all settings and have the most consistently strong effects. TKN estimates for the two locations just upstream of LD1 are all positive, while the P estimates from the same locations are all negative.

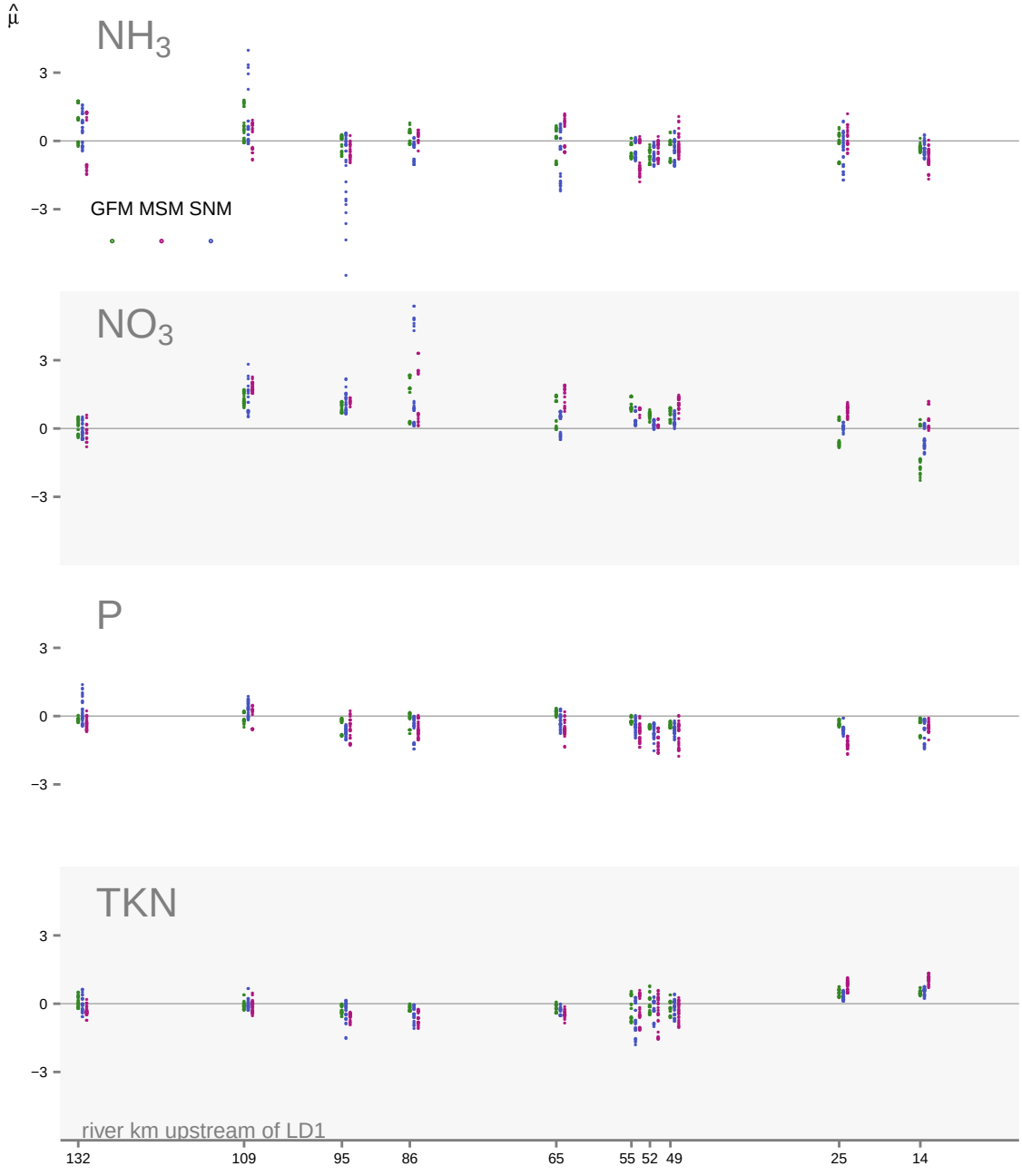

Figure 2: Volcano plot of estimates of the Cape Fear analysis showing significance and estimates for all analysis methods and models. The point estimates are same in all the panels. Significance levels vary depending on the distribution used for the test statistic.

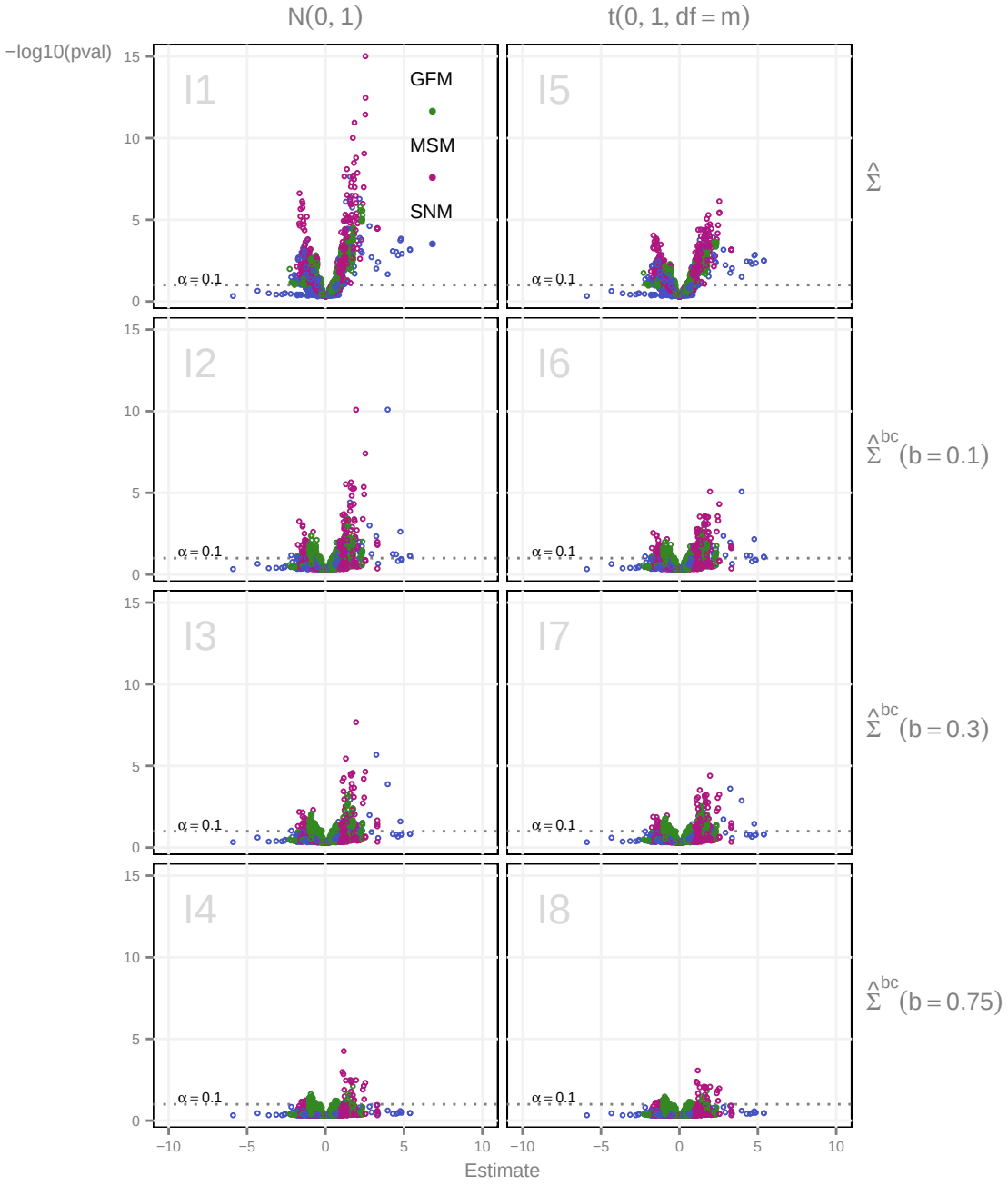

Figure 3: This figure repeats main text Figure 5 with estimates based on the estimated derived from 5 imputed datasets. These results are largely substantively the same as those reported in main text Figure 5.